A Homozygous Missense Mutation in the *IRBP* Gene (*RBP3*) Associated with Autosomal Recessive Retinitis Pigmentosa

Anneke I. den Hollander[1,2], **Terri L. McGee**[1], **Carmela Ziviello**[3,4], **Sandro Banfi**[3], **Thaddeus P. Dryja**[5], **Federico Gonzalez-Fernandez**[6,7,8], **Debashis Ghosh**[9,10], and **Eliot L. Berson**[1]

[1]The Berman-Gund Laboratory for the Study of Retinal Degenerations, Harvard Medical School, Massachusetts Eye and Ear Infirmary, Boston, Massachusetts

[3]Téléthon Institute of Genetics and Medicine, Naples, Italy

[4]Institute of Genetics and Biophysics "A. Buzzati-Traverso", CNR (Consiglio Nazionale delle Ricerche, Naples, Italy

[5]Ocular Molecular Genetics Institute, Harvard Medical School, Massachusetts Eye and Ear Infirmary, Boston, Massachusetts

[6]Research Service, Veterans Affairs Medical Center, Buffalo, New York

[7]The Department of Ophthalmology, State University of New York, Buffalo, New York

[8]The Department of Pathology, Ross Eye Institute, State University of New York, Buffalo, New York

[9]Structural Biology Department of the University at Buffalo, Hauptman-Woodward Institute, Buffalo, New York

[10]Program of Molecular Pharmacology and Therapeutics, Roswell Park Cancer Institute, Buffalo, New York.

Abstract

PURPOSE—Interphotoreceptor retinoid-binding protein (IRBP) has been considered essential for normal rod and cone function, as it mediates the transport of retinoids between the photoreceptors and the retinal pigment epithelium. This study was performed to determine whether mutations in the *IRBP* gene (*RBP3*) are associated with photoreceptor degeneration.

METHODS—A consanguineous family was ascertained in which four children had autosomal recessive retinitis pigmentosa (RP). Homozygosity mapping performed with SNP microarrays revealed only one homozygous region shared by all four affected siblings. Sequencing of *RBP3*, contained in this region, was performed in this family and others with recessive RP. Screening was also performed on patients with various other forms of retinal degeneration or malfunction.

RESULTS—Sequence analysis of *RBP3* revealed a homozygous missense mutation (p.Asp1080Asn) in the four affected siblings. The mutation affects a residue that is completely conserved in all four homologous modules of the IRBP protein of vertebrate species and in C-terminal-processing proteases, photosynthesis enzymes found in bacteria, algae, and plants. Based

on the previously reported crystal structure of *Xenopus* IRBP, the authors predict that the Asp1080-mediated conserved salt bridge that appears to participate in scaffolding of the retinol-binding domain is abolished by the mutation. No *RBP3* mutations were detected in 395 unrelated patients with recessive or isolate RP or in 680 patients with other forms of hereditary retinal degeneration.

CONCLUSIONS—Mutations in *RBP3* are an infrequent cause of autosomal recessive RP. The mutation Asp1080Asn may alter the conformation of the IRBP protein by disrupting a conserved salt bridge.

Interphotoreceptor retinoid-binding protein (IRBP) is specifically expressed by the photoreceptors and is the most abundant protein in the interphotoreceptor matrix.[1−4] IRBP may have a role in the transport of visual cycle retinoids between the photoreceptor outer segments and the retinal pigment epithelium and possibly the Müller cells.[5−9] During the transport process IRBP protects retinol from isomerization and oxidation.[10] Besides its role in the visual cycle, IRBP also binds fatty acids,[11,12] and it may be involved in retinal development. [13,14]

IRBP consists of four tandem homologous modules, each spanning approximately 300 amino acids. Each module has retinoid-binding activity in biochemical assays. However, recent studies of *Xenopus* IRBP suggest that one four-module IRBP molecule contains only one retinol-binding site.[15] It remains to be determined whether the retinol-binding pocket is restricted to one of the four modules or to an intramodule site defined by multiple modules.

Transgenic mice with a targeted disruption of the *Irbp* gene exhibit a significant loss of photoreceptors as well as profound changes in the structure and organization of the outer segments, even before their eyes have opened.[14] Consistent with these observations, electroretinographic recordings in 1-month-old $Irbp^{-/-}$ mice show a marked reduction of the rod-mediated and cone-mediated response amplitudes. Initially no evidence of gross abnormalities in the visual cycle in $Irbp^{-/-}$ mice were found,[16,17] but more recent studies suggest that a defect in the visual cycle is present (Parker RO, et al. *IOVS*. 2008;49:ARVO E-Abstract 3524).[18]

So far, no human disease has been associated with mutations in the *IRBP* gene (*RBP3*). We present a consanguineous family with recessive retinitis pigmentosa (RP) that may be the first identified with a pathogenic IRBP mutation.

MATERIALS AND METHODS

This study was conducted according to the tenets of the Declaration of Helsinki. Approval was obtained from the Internal Review Boards of the Massachusetts Eye and Ear Infirmary, Harvard Medical School, and the Téléthon Institute of Genetics and Medicine. Informed consent was obtained from all the participants.

Clinical Evaluation

Two of the affected siblings from a consanguineous Italian family had ocular examinations in the Berman-Gund Laboratory at the Massachusetts Eye and Ear Infirmary, including measurement of best-corrected visual acuity on a Snellen chart, slit lamp biomicroscopy, and ophthalmoscopy. Fundus photographs were also obtained. Color vision was tested with the Farnsworth-D-15 panel. Dark adaptation testing was performed with a Goldmann-Weekers adaptometer after 45 minutes of dark adaptation to an 11° white test light fixated centrally or 7° above fixation. Kinetic visual fields were measured with the Goldmann perimeter to the V-4e and I-4e white test lights against the standard white background of 31.5 apostilbs. Field areas contiguous to the center (i.e., excluding peripheral islands) were plotted with a digitizing tablet or scanned by custom software and converted to areas in degrees squared as described

previously.[19] A contact lens electrode was placed on the topically anesthetized cornea, and full-field electroretinograms (ERGs) were elicited with 0.5-Hz flashes of dim blue light, 0.5-Hz flashes of white light, and 30-Hz white flickering light after pupillary dilation and 45 minutes of dark adaptation. In patients with 30-Hz responses <10 µV the responses were computer averaged and narrow band-pass filtered as also described previously.[19–21] Retinal thickness was measured by optical coherence tomography (OCT). The other two affected siblings were clinically evaluated in Italy by ophthalmoscopy and electroretinography.

Molecular Genetic Analysis

Blood samples were obtained from patients and their family members. Leukocyte DNA was extracted using standard procedures. DNA samples of two affected individuals from a consanguineous Italian family with autosomal recessive RP were genotyped for 262,000 single-nucleotide polymorphisms (SNPs; GeneChip Mapping 250K Nsp Array; Affymetrix, Santa Clara, CA) at the Microarray Core of the Dana-Farber Cancer Institute. The genotyping data were analyzed for homozygous regions using dCHIP.[22] Regions that were homozygous in both individuals were analyzed with selected SNPs in the entire family by direct sequencing. Direct sequencing was performed on an automated sequencer (model 3100; Applied Biosystems, Inc. [ABI], Foster City, CA) with sequence analysis software (Vector NTI Advance, ver. 10; Invitrogen Corp., Carlsbad, CA).

Positional candidate genes were selected from the UCSC Human Genome Browser, March 2006 Assembly (University of California, Santa Cruz, CA). Expression profiles of these genes were evaluated with the Unigene database ((http://www.ncbi.nlm.nih.gov/UniGene; provided in the public domain by the National Center for Biotechnology Information, Bethesda, MD). The phenotypes of available knock-out mice were assessed through the Mouse Genome Database (Jackson Laboratory, Bar Harbor, ME). Primer pairs were selected to amplify the coding sequence as well as intron DNA flanking the exons of candidate genes. Primers used to amplify the four exons of *RBP3* are listed in Table 1. All members of this consanguineous family were analyzed for mutations in *RBP3* by direct sequencing. *RBP3* was also analyzed in DNA samples of 289 probands with autosomal recessive RP, 106 isolate patients with RP, 103 probands with autosomal dominant RP, 98 probands with cone–rod dystrophy (CRD), 41 patients with Leber congenital amaurosis (LCA), and 438 patients with other retinal degenerations and malfunctions, either by direct sequencing or by single-strand conformation polymorphism analysis. Exon 2 of *RBP3* (which contains residue Asp1080) was analyzed in 367 additional patients with autosomal recessive or isolate RP (including 179 Italian patients). DNA samples from 94 normal subjects of mixed North American ethnicity and from 116 normal Italian subjects were also screened.

Structural Modeling

Currently, the only known x-ray crystal structure of IRBP is that of the second module of *Xenopus* IRBP (X2IRBP).[23] Asp462 is the amino acid residue in X2IRBP that corresponds to Asp1080 in the fourth module of human IRBP. To show the relationship of this aspartic acid residue to the potential retinoid-binding site, in silico docking of all-*trans* retinol to X2IRBP was accomplished using the Molecular Operating Environment (MOE 2005.08; Chemical Computing Group, Montreal, Quebec, Canada).[24,25] The site finder option of MOE, which automatically identifies internal cavities within a receptor protein was previously used to locate possible ligand-binding sites in the X2IRBP crystal structure (pdb code: 1J7X).[23] In this analysis, partial charges of the amino acids and the ligand were accounted for, and full conformational searches for the ligand were made. The pose with the best score was selected as the model for the docked ligand. To account for conformational flexibility of the active site pocket, the immediate neighborhood of the retinol-binding site (within 4.5 Å of the ligand) was energy minimized by restrained minimization.[25] A molecular visualization system

PyMOL (open source software published by DeLano Scientific LLL; Palo Alto, CA) was used to depict in stereo view the relative position of Asp462 with the retinoid-binding site and salt bridge with Arg464.

RESULTS

Homozygosity mapping was performed in the Italian consanguineous family with autosomal recessive RP to identify the genetic defect causing the disease. Two affected individuals (II-3 and II-4) were genotyped with 262,000 SNPs. Two shared homozygous regions were identified in these individuals: a 6-Mb region on chromosome 20 containing 520 homozygous SNPs and a 40-Mb region on chromosome 10 spanning 3780 SNPs. Haplotype analysis in all family members excluded the involvement of the chromosome 20 region, since one of the affected individuals (II-1) was not homozygous for alleles in this interval. The haplotypes at the locus on chromosome 10 completely segregated with the disease in this family. Two recombination events were observed, which reduced the critical interval to 9 Mb between SNPs rs2460551 and rs7898315 (Fig. 1A).

This interval contains 57 annotated genes. All genes in the region were evaluated as candidates for disease by assessment of their expression pattern, function, and the phenotype of available targeted knockout mice. Twenty-three genes are not expressed in the eye, 29 genes are expressed in the eye but also broadly in other tissues, and 4 genes (*CHAT*, *FRMPD2*, *GDF10*, and *SLC18A3*) are expressed in the eye and only a small number of other tissues. *RBP3* was considered to be the best candidate gene in the region because it is the only gene that is highly and exclusively expressed in the retina. In addition, the photoreceptor degeneration observed in transgenic *Irbp*^{−/−} mice[14] correlates with the disease in this family. *Chat*^{−/−} and *Slc18a3*^{−/−} mice have severe neuromuscular deficits[26–28] and were therefore excluded as candidate genes. Although it is ubiquitously expressed, the oxoglutarate dehydrogenase-like (*OGDHL*) gene was considered to be a functional candidate gene for RP, since oxoglutarate dehydrogenase is the enzyme that catalyzes the conversion of 2-oxoglutarate to succinyl-coA and CO_2 within the Krebs cycle. This is the step after the IDH3 reaction, which was recently found to be associated with RP.[29]

Sequence analysis of the *GDF10* gene in an affected individual did not reveal any sequence changes. The individual was homozygous for the "A" allele of a previously documented SNP in the *OGDHL* gene (rs7090775; c.657G>A; p.Gln219Gln). The individual was apparently heterozygous at three SNPs in the *FRMPD2* gene: c.2620A>G, Ser874Gly (SNP rs1346694); c.2889T>C, Ser963Ser (SNP rs2579678); and c.2902A>G; Ile968Val. The heterozygous state of the changes identified in the *FRMPD2* gene is inconsistent with the homozygosity of the entire region in the patients. It is explained because this gene is located in a portion of the chromosome known to have undergone a segmental duplication and the primers used to amplify the gene most likely coamplify two or more regions of nearly identical sequence. None of the changes found were deemed pathogenic as most are known SNPs and the Ile968Val change was also found in a normal control.

Sequence analysis of the *RBP3* gene identified a homozygous missense mutation (c.3238G>A, p.Asp1080Asn) in exon 2 in all affected individuals (Fig. 1B). The p.Asp1080Asn mutation was not observed in 762 unrelated probands with autosomal recessive or isolate RP, including 179 Italian probands, nor was it found among 94 unaffected control subjects of mixed North American ethnicity or 116 Italian control subjects without known photoreceptor disease. Asp1080 is located in the fourth IRBP repeat module, and the homologous residue is completely identical among all four IRBP modules of vertebrate species (Fig. 2). The IRBP protein sequence and structure show similarity to a family of enzymes called C-terminal-processing proteases, which are part of the photosynthetic system in bacteria, algae, and plants.

[13,30–32] The homologous aspartic acid is also identical among C-terminal processing proteases from these distant species, demonstrating that it is highly conserved during evolution (Fig. 2). IRBP has been found to have structural homology with the enoyl Co-A hydratase/isomerase superfamily by using three-dimensional search programs, but the sequence identity was reported to be low.[23] It is, therefore, not surprising that Asp1080 is not conserved among that family.

Detailed clinical evaluations were performed on two of the four affected patients of this family in the Berman-Gund Laboratory (II-1 and II-3; Table 2, Fig. 3). Patient II-3 reported loss of central vision and onset of nightblindness at age 32, whereas patient II-1 reported loss of central vision at age 60 and no night deficiency even at age 67. Patient II-1 had visual acuities of 20/60 and 20/80 at age 67, and patient II-3 had acuities of 20/200 in each eye at age 46. Patient II-1 had normal color vision on the Farnsworth-D-15 panel, and patient II-3 had a tritan axis of confusion on this test. The visual fields showed a marked constriction with the I-4e and a midperipheral scotoma with the V-4e test light in both patients. The visual fields were more severely diminished in patient II-3 at age 46 than in patient II-1 at age 67. Both patients showed clumped and bone spicule pigment around the periphery. Patient II-3 had waxy pallor of the optic disc and attenuated retinal vessels. Patient II-1 had normal color in each disc with a large area of atrophy just temporal to each disc and had attenuated retinal vessels. The central macula in each patient retained a normal or near-normal color. Both patients had posterior subcapsular cataracts at the first visit. Patient II-3 subsequently had cataract surgery with posterior chamber lens implants. The ERGs in both patients showed a profound loss of rod and cone function. Cone ERG amplitudes of both patients were substantially smaller than normal and could be detected only by computer averaging and narrow band-pass filtering. Cone amplitudes were smaller in patient II-3 at age 46 than in patient II-1 at age 67 (Table 2, Fig. 3). The delayed cone implicit times were compatible with progressive disease.[33] The other two affected siblings (patients II-2 and II-4) were examined in Italy and were reported to have fundus findings of RP by ophthalmoscopy and very reduced ERG responses that were virtually nondetectable without computer averaging. The unaffected sibling (individual II-5) had no symptoms or signs of RP. The parents had died in later life and had no visual symptoms.

Patient II-3 had reduced central retinal thickness on OCT and patient II-1 had increased macular thickness due to cystoid macular edema as possible explanations for their decreased acuities. Patient II-3 was evaluated at several time points which permitted an analysis of the progression of visual decline (Table 2). He began treatment with vitamin A palmitate, 15,000 IU/d after his second examination. The annual decline of his remaining visual field area contiguous to the center was 5.4%, and the annual decline in his remaining cone ERG amplitude was 4.4%, with both values being averages across both eyes. The rates of decline of the remaining field area and cone ERG amplitude were slower, respectively, than the average rates of 7.2% and 10% per year reported for patients with typical RP who were not receiving treatment and had been tested in the same way.[19]

To further examine the structural consequences of substituting Asn for the residue Asp1080, we used the x-ray crystallographic structure of the second module of *Xenopus* IRBP (X2IRBP). [23] Currently, the only known crystal structure for IRBP is that of X2IRBP. Although Asp1080 is located in the fourth module of human IRBP, this Asp is strictly conserved among all modules in all IRBPs (Fig. 2). Furthermore, homology modeling and biochemical studies indicate that the individual modules are remarkably conserved and represent functional units of the protein. [25,34]

Figure 4 shows a ribbon representation of the x-ray crystal structure of X2IRBP, in which an all-*trans* retinol molecule (magenta) is docked into the putative binding site.[25] Asp1080 in human IRBP corresponds to Asp462 in X2IRBP. Of particular interest is the presence of a

nearby arginine residue, Arg464 (corresponding to Arg1082 in module 4 of human IRBP). The crystal structure indicates that Asp462 and Arg464 participate in the formation of a salt bridge. A further remarkable feature of the structure is the close proximity (~9 Å) of Asp462 with the cyclohexane ring of bound retinol (Fig. 4B). Asp462 appears to participate in the scaffold of the retinol-binding domain.

Previous studies have called attention to conserved boxes in the primary structure of IRBP. [35] The most highly conserved of these contains the Asp1080 residue, as well as several other residues including Arg1082. Substitution of asparagine (Asn) for aspartic acid (Asp) at codon 1080 would disrupt this interaction. Asp and Asn belong to different biochemical classes of amino acid residues. Asp has a carboxyl group that is negatively charged at neutral pH and is thus capable of forming a salt bridge with a positively charged arginine guanidinium group. In contrast, the Asn side chain has a neutral carboxamide group that is unable to form a salt bridge. The highly conserved Asp-Arg salt bridge would therefore be abolished by the Asp1080Asn mutation.

The entire coding region of *RBP3* was additionally analyzed in DNA samples of 289 probands with autosomal recessive RP and 106 isolate patients with RP. In addition, 103 probands with autosomal dominant RP, 98 probands with CRD, 41 patients with LCA, and 438 patients with various retinal degenerations and malfunctions were analyzed. A heterozygous nonsense mutation (c.1216G>T, p.Glu406X) was identified in an isolate patient with sector RP. His unaffected brother also carried the nonsense mutation and had the same haplotype on the other allele (Fig. 5). The brother and carrier mother were examined and had normal fundi, ERGs, and visual fields thereby excluding *RBP3* as a cause of recessive or dominant disease in this family.

In addition, 23 synonymous and 40 nonsynonymous changes were identified among these 1075 probands (Table 3, Table 4). Three variants (p.Thr279Thr, p.Leu699Leu, and p.Val884Met) were known SNPs. Fourteen variants (p.Gly272Gly, p.Pro281Pro, p.Pro308Pro, p.Arg346His, p.Arg544His, p.Ala688Val, p.Val693Met, p.Pro723Leu, p.Asp749Asp, p.Arg833Cys, p.Tyr952Tyr, p.Ser966Ser, p.His1182His, and p.Thr1194Met) were found in more than one patient with different clinical diagnoses, and therefore likely represent rare nonpathogenic variants. For nine variants (p.Ser163Pro, p.Arg267Gln, p.Val282Met, p.Arg544His, p.Val593Ala, p.Ala688Val, p.Arg747Cys, p.Asn785Lys, and p.Arg833Cys) pathogenicity was excluded because the variant did not segregate with the disease in the family. The nonsynonymous changes did not affect any of the residues that are conserved among all IRBP modules of vertebrates and C-terminal- processing proteases of bacteria, algae, and plants. All these variants were detected infrequently in only one or two patients and were all found in the heterozygous state. None of the patients carrying these changes had a second heterozygous change that could be located on the other allele except one isolate patient with RP who was heterozygous for p.Glu956Lys and p.Val1059Ile. Family members of this patient were not available, and it could therefore not be determined whether these variants were allelic or syntenic.

DISCUSSION

Targeted knockout of the *Irbp* gene causes photoreceptor degeneration in mice,[14] but no human disease has so far been associated with mutations in this gene. In this study, we identified a family with autosomal recessive RP in which a missense mutation (p.Asp1080Asn) in *RBP3* cosegregates with the disease. Patient II-3 was more severely affected at age 46 than his older brother (II-1) was at age 67, demonstrating a wide range of severity in this family. Patient II-3 had much slower rates of field and ERG loss than the average rates previously reported for typical untreated RP.[19] He was being treated with vitamin A palmitate between his second and

third visits (15,000 IU/d), which may have slowed the course of the disease. It is of interest that administration of 9-*cis* retinal has resulted in an improvement of cone function in *Irbp*$^{-/-}$ mice (Parker RO, et al. *IOVS*. 2008;49:ARVO E-Abstract 3524). A more severe cone than rod degeneration was recently reported in *Irbp*$^{-/-}$ mice (Parker RO, et al. *IOVS*. 2008;49:ARVO E-Abstract 3524),[18] but we could not ascertain whether patients II-1 and II-3 had predominant loss of cone or rod function when they presented with moderately advanced stages of their disease.

The Asp1080Asn mutation detected in this family points to a key role of conserved Asp-Arg salt bridges in IRBP. Although the exact role of Asp1080 or the salt bridge is unknown at the present time, some possible functions should be considered. Since Asp1080 appears to participate in the scaffold forming the ligand-binding domain for all-*trans* retinol, it is possible that breaking the salt bridge may affect the structure of the ligand-binding site altering the binding affinity. There are few data in the literature to evaluate this possibility. However, a conservative substitution of the Arg side chain for a Gln in module 4 of *Xenopus* IRBP does not significantly alter binding of all-*trans* retinol.[36]

The Asp-Arg salt bridge may mediate intramolecular and/or intermolecular interactions important to regulate the binding, protection, or release of visual cycle retinoids by IRBP. In the original description of the crystal structure of X2IRBP, attention was called to the conserved Arg residues clustering in a solvent-exposed region. In other proteins, surface salt bridges are less likely to simply support protein stability.[37] For IRBP, one possibility is that the Asp and/ or Arg residues mediate intermolecular interactions. Such interactions could involve the binding with cell surface receptor(s) or molecular component(s) of the interphotoreceptor matrix.

It should also be pointed out that the existing structural data are based on only a single module of IRBP. Therefore, the Asp and/or Arg residue could be involved in interactions between modules. Such an interaction could be analogous to the intermolecular salt bridges required for activation of specific protein kinases.[38] In that system, kinase dimerization occurs via interface salt bridge formation between an Arg from one protomer and the Asp of another protomer (where a protomer is the smallest subset of subunits comprising an oligomer). It should be kept in mind that Asp-Arg salt bridges can have diverse roles including receptor recognition,[39] ligand-binding, [40·41] and intramolecular interactions promoting folding and stability.[42,43] Crystallography of Asp to Asn mutants of both ribulose-1,5-bisphosphate carboxylase and chloramphenicol acetyltransferase have shown that specific Asp to Asn substitutions disrupt a salt bridge and dramatically alter protein conformation, resulting in greatly reduced function.[44,45] Although the exact role of the salt bridge in IRBP is unknown, the Asp1080Asn mutation in the family described herein points to the disruption of charge neutralization between two side chains near the ligand-binding site, with possible functional implications. A more precise model of the functional consequence of this mutation necessitates the future isolation and structural analysis of the full-length IRBP and biochemical analysis of the mutant protein.

We found that *RBP3* mutations are not commonly associated with autosomal recessive RP, since an analysis of 395 additional families with recessive or isolate RP found no others with clearly associated *RBP3* mutations. One heterozygous nonsense mutation (p.Glu406X) was identified in an isolate patient with sector RP, but autosomal recessive and autosomal dominant inheritance of *RBP3* alleles was excluded. There remains the possibility that this patient carries a mutation in another gene, leading to disease by a digenic inheritance mechanism.

Acknowledgments

References

1. Adler AJ, Martin KJ. Retinol-binding proteins in bovine interphotoreceptor matrix. Biochem Biophys Res Commun 1982;108:1601–1608. [PubMed: 6891215]

2. Bunt-Milam AH, Saari JC. Immunocytochemical localization of two retinoid-binding proteins in vertebrate retina. J Cell Biol 1983;97:703–712. [PubMed: 6350319]

3. Gonzalez-Fernandez F, Landers RA, et al. An extracellular retinol-binding glycoprotein in the eyes of mutant rats with retinal dystrophy: development, localization, and biosynthesis. J Cell Biol 1984;99:2092–2098. [PubMed: 6389570]

4. Pfeffer B, Wiggert B, Lee L, Zonnenberg B, Newsome D, Chader G. The presence of a soluble interphotoreceptor retinol-binding protein (IRBP) in the retinal interphotoreceptor space. J Cell Physiol 1983;117:333–341. [PubMed: 6686234]

5. Liou GI, Bridges CD, Fong SL, Alvarez RA, Gonzalez-Fernandez F. Vitamin A transport between retina and pigment epithelium-an interstitial protein carrying endogenous retinol (interstitial retinolbinding protein). Vision Res 1982;22:1457–1467. [PubMed: 6892133]

6. Lai YL, Wiggert B, Liu YP, Chader GJ. Interphotoreceptor retinol-binding proteins: possible transport vehicles between compartments of the retina. Nature 1982;298:848–849. [PubMed: 7202123]

7. Fong SL, Liou GI, Landers RA, Alvarez RA, Bridges CD. Purification and characterization of a retinol-binding glycoprotein synthesized and secreted by bovine neural retina. J Biol Chem 1984;259:6534–6542. [PubMed: 6427217]

8. Mata NL, Radu RA, Clemmons RC, Travis GH. Isomerization and oxidation of vitamin A in cone-dominant retinas: a novel pathway for visual-pigment regeneration in daylight. Neuron 2002;36:69–80. [PubMed: 12367507]

9. Wu Q, Blakeley LR, Cornwall MC, Crouch RK, Wiggert BN, Koutalos Y. Interphotoreceptor retinoid-binding protein is the physiologically relevant carrier that removes retinol from rod photoreceptor outer segments. Biochemistry 2007;46:8669–8679. [PubMed: 17602665]

10. Crouch RK, Hazard ES, Lind T, Wiggert B, Chader G, Corson DW. Interphotoreceptor retinoid-binding protein and α-tocopherol preserve the isomeric and oxidation state of retinol. Photochem Photobiol 1992;56:251–255. [PubMed: 1502268]

11. Semenova EM, Converse CA. Comparison between oleic acid and docosahexaenoic acid binding to interphotoreceptor retinoid-binding protein. Vision Res 2003;43:3063–3067. [PubMed: 14611942]

12. Bazan NG, Reddy TS, Redmond TM, Wiggert B, Chader GJ. Endogenous fatty acids are covalently and noncovalently bound to interphotoreceptor retinoid-binding protein in the monkey retina. J Biol Chem 1985;260:13677–13680. [PubMed: 3932343]

13. Gonzalez-Fernandez F. Interphotoreceptor retinoid-binding protein: an old gene for new eyes. Vision Res 2003;43:3021–3036. [PubMed: 14611938]

14. Liou GI, Fei Y, Peachey NS, et al. Early onset photoreceptor abnormalities induced by targeted disruption of the interphotoreceptor retinoid-binding protein gene. J Neurosci 1998;18:4511–4520. [PubMed: 9614228]

15. Ghosh D, Griswold JB, Bevilacqua T, Gonzalez-Fernandez F. Purification of the full-length *Xenopus* interphotoreceptor retinoid binding protein and growth of diffraction-quality crystals. Mol Vis 2007;13:2275–2281. [PubMed: 18079675]

16. Palczewski K, Van Hooser JP, Garwin GG, Chen J, Liou GI, Saari JC. Kinetics of visual pigment regeneration in excised mouse eyes and in mice with a targeted disruption of the gene encoding

interphotoreceptor retinoid-binding protein or arrestin. Biochemistry 1999;38:12012–12019. [PubMed: 10508404]

17. Ripps H, Peachey NS, Xu X, Nozell SE, Smith SB, Liou GI. The rhodopsin cycle is preserved in IRBP "knockout" mice despite abnormalities in retinal structure and function. Vis Neurosci 2000;17:97–105. [PubMed: 10750831]

18. Jin M, Li S, Nusinowitz S, et al. The role of interphotoreceptor retinoid-binding protein on the translocation of visual retinoids and function of cone photoreceptors. J Neurosci 2009;29:1486–1495. [PubMed: 19193895]

19. Berson EL, Rosner B, Sandberg MA, et al. A randomized trial of vitamin A and vitamin E supplementation for retinitis pigmentosa. Arch Ophthalmol 1993;111:761–772. [PubMed: 8512476]

20. Andreasson SO, Sandberg MA, Berson EL. Narrow-band filtering for monitoring low-amplitude cone electroretinograms in retinitis pigmentosa. Am J Ophthalmol 1988;105:500–503. [PubMed: 3285692]

21. Berson EL. Long-term visual prognoses in patients with retinitis pigmentosa: the Ludwig von Sallmann lecture. Exp Eye Res 2007;85:7–14. [PubMed: 17531222]

22. Lin M, Wei LJ, Sellers WR, Lieberfarb M, Wong WH, Li C. dChipSNP: significance curve and clustering of SNP-array-based loss-of-heterozygosity data. Bioinformatics 2004;20:1233–1240. [PubMed: 14871870]

23. Loew A, Gonzalez-Fernandez F. Crystal structure of the functional unit of interphotoreceptor retinoid binding protein. Structure 2002;10:43–49. [PubMed: 11796109]

24. Gonzalez-Fernandez F, Ghosh D. Focus on molecules: interphotoreceptor retinoid-binding protein (IRBP). Exp Eye Res 2008;86:169–170. [PubMed: 17222825]

25. Gonzalez-Fernandez F, Baer CA, Ghosh D. Module structure of interphotoreceptor retinoid-binding protein (IRBP) may provide bases for its complex role in the visual cycle: structure/function study of *Xenopus* IRBP. BMC Biochem 2007;8:15. [PubMed: 17683573]

26. Prado VF, Martins-Silva C, de Castro BM, et al. Mice deficient for the vesicular acetylcholine transporter are myasthenic and have deficits in object and social recognition. Neuron 2006;51:601–612. [PubMed: 16950158]

27. Misgeld T, Burgess RW, Lewis RM, Cunningham JM, Lichtman JW, Sanes JR. Roles of neurotransmitter in synapse formation: development of neuromuscular junctions lacking choline acetyltransferase. Neuron 2002;36:635–648. [PubMed: 12441053]

28. Brandon EP, Lin W, D'Amour KA, et al. Aberrant patterning of neuromuscular synapses in choline acetyltransferase-deficient mice. J Neurosci 2003;23:539–549. [PubMed: 12533614]

29. Hartong DT, Dange M, McGee TL, Berson EL, Dryja TP, Colman RF. Insights from retinitis pigmentosa into the roles of isocitrate dehydrogenases in the Krebs cycle. Nat Genet 2008;40:1230–1234. [PubMed: 18806796]

30. Baer CA, Retief JD, Van NE, Braiman MS, Gonzalez-Fernandez F. Soluble expression in *E. coli* of a functional interphotoreceptor retinoid-binding protein module fused to thioredoxin: correlation of vitamin A binding regions with conserved domains of C-terminal processing proteases. Exp Eye Res 1998;66:249–262. [PubMed: 9533851]

31. Loew A, Baer C, Gonzalez-Fernandez F. The functional unit of interphotoreceptor retinoid-binding protein (IRBP): purification, characterization and preliminary crystallographic analysis. Exp Eye Res 2001;73:257–264. [PubMed: 11446776]

32. Gonzalez-Fernandez F. Evolution of the visual cycle: the role of retinoid-binding proteins. J Endocrinol 2002;175:75–88. [PubMed: 12379492]

33. Berson EL. Retinitis pigmentosa. The Friedenwald Lecture. Invest Ophthalmol Vis Sci 1993;34:1659–1676. [PubMed: 8473105]

34. Nickerson JM, Li GR, Lin ZY, Takizawa N, Si JS, Gross EA. Structure-function relationships in the four repeats of human interphotoreceptor retinoid-binding protein (IRBP). Mol Vis 1998;4:33. [PubMed: 9873071]

35. Rajendran RR, Van Niel EE, Stenkamp DL, Cunningham LL, Raymond PA, Gonzalez-Fernandez F. Zebrafish interphotoreceptor retinoid-binding protein: differential circadian expression among cone subtypes. J Exp Biol 1996;199:2775–2787. [PubMed: 9110959]

36. Baer CA, Van Niel EE, Cronk JW, et al. Arginine to glutamine substitutions in the fourth module of *Xenopus* interphotoreceptor retinoid-binding protein. Mol Vis 1998;4:30. [PubMed: 9873068]

37. Takano K, Tsuchimori K, Yamagata Y, Yutani K. Contribution of salt bridges near the surface of a protein to the conformational stability. Biochemistry 2000;39:12375–12381. [PubMed: 11015217]

38. Dey M, Cao C, Sicheri F, Dever TE. Conserved intermolecular salt bridge required for activation of protein kinases PKR, GCN2, and PERK. J Biol Chem 2007;282:6653–6660. [PubMed: 17202131]

39. Peschard P, Ishiyama N, Lin T, Lipkowitz S, Park M. A conserved DpYR motif in the juxtamembrane domain of the Met receptor family forms an atypical c-Cbl/Cbl-b tyrosine kinase binding domain binding site required for suppression of oncogenic activation. J Biol Chem 2004;279:29565–29571. [PubMed: 15123609]

40. Fuentes-Prior P, Noeske-Jungblut C, Donner P, Schleuning WD, Huber R, Bode W. Structure of the thrombin complex with triabin, a lipocalin-like exosite-binding inhibitor derived from a triatomine bug. Proc Natl Acad Sci U S A 1997;94:11845–11850. [PubMed: 9342325]

41. Stockner T, Vogel HJ, Tieleman DP. A salt-bridge motif involved in ligand binding and large-scale domain motions of the maltose-binding protein. Biophys J 2005;89:3362–3371. [PubMed: 16143635]

42. Kursula I, Partanen S, Lambeir AM, Wierenga RK. The importance of the conserved Arg191-Asp227 salt bridge of triosephosphate isomerase for folding, stability, and catalysis. FEBS Lett 2002;518:39–42. [PubMed: 11997014]

43. Lewendon A, Murray IA, Kleanthous C, Cullis PM, Shaw WV. Substitutions in the active site of chloramphenicol acetyltransferase: role of a conserved aspartate. Biochemistry 1988;27:7385–7390. [PubMed: 3061455]

44. Soderlind E, Schneider G, Gutteridge S. Substitution of ASP193 to ASN at the active site of ribulose-1,5-bisphosphate carboxylase results in conformational changes. Eur J Biochem 1992;206:729–735. [PubMed: 1606957]

45. Gibbs MR, Moody PC, Leslie AG. Crystal structure of the aspartic acid-199-asparagine mutant of chloramphenicol acetyltransferase to 2.35-A resolution: structural consequences of disruption of a buried salt bridge. Biochemistry 1990;29:11261–11265. [PubMed: 2271709]
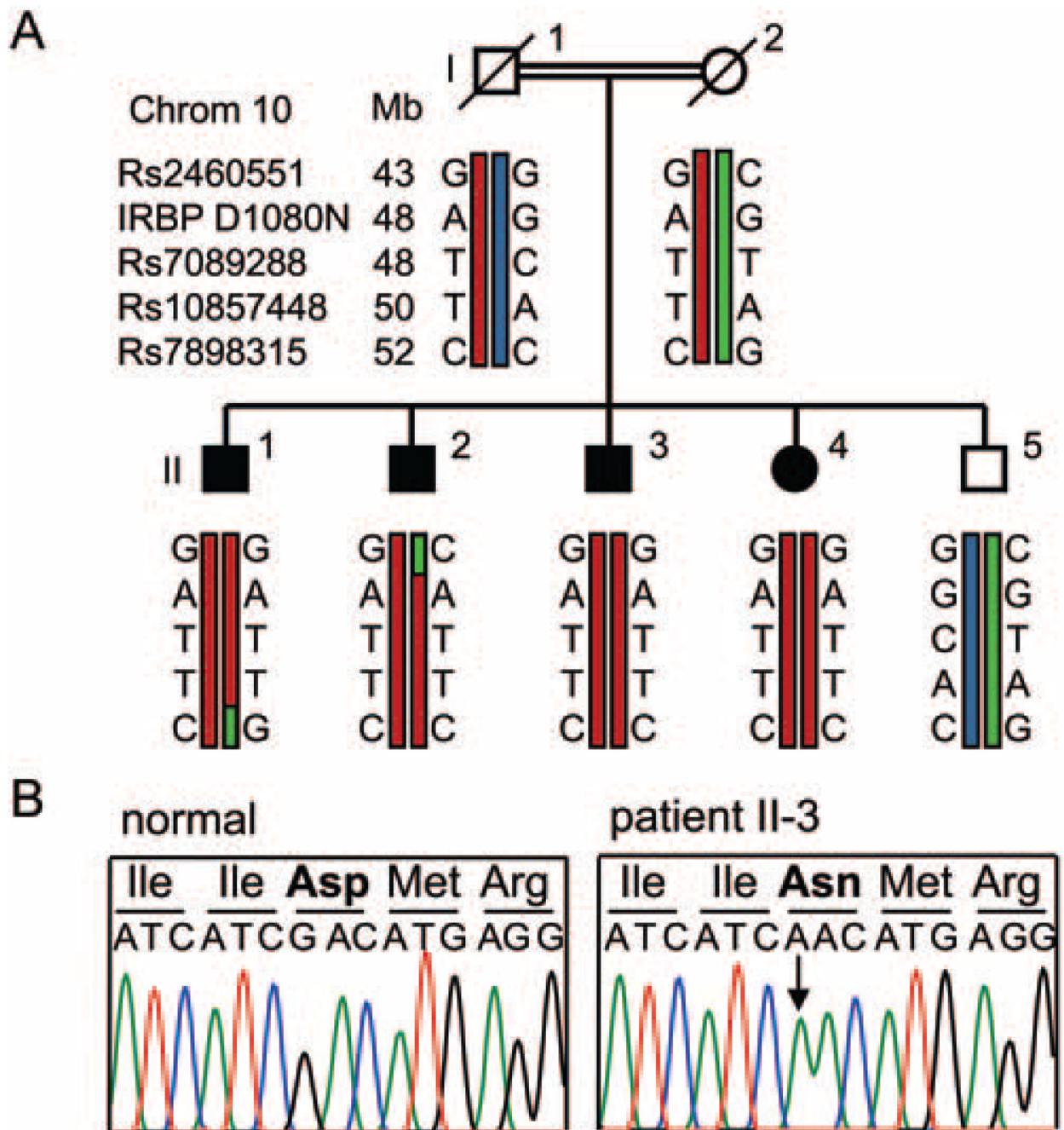
Figure 1.
Molecular genetic analysis in a consanguineous family with autosomal recessive RP. (**A**) Pedigree of the family; the parents were first cousins and had no history of visual loss. All four affected siblings shared a 9-Mb homozygous region on chromosome 10, whereas the unaffected sibling was not homozygous for alleles in this interval. (**B**) Sequence analysis of *RBP3* identified a homozygous missense mutation (c.3238G>A, p.Asp1080Asn) in exon 2 in all affected individuals. *Arrow*: mutant base.
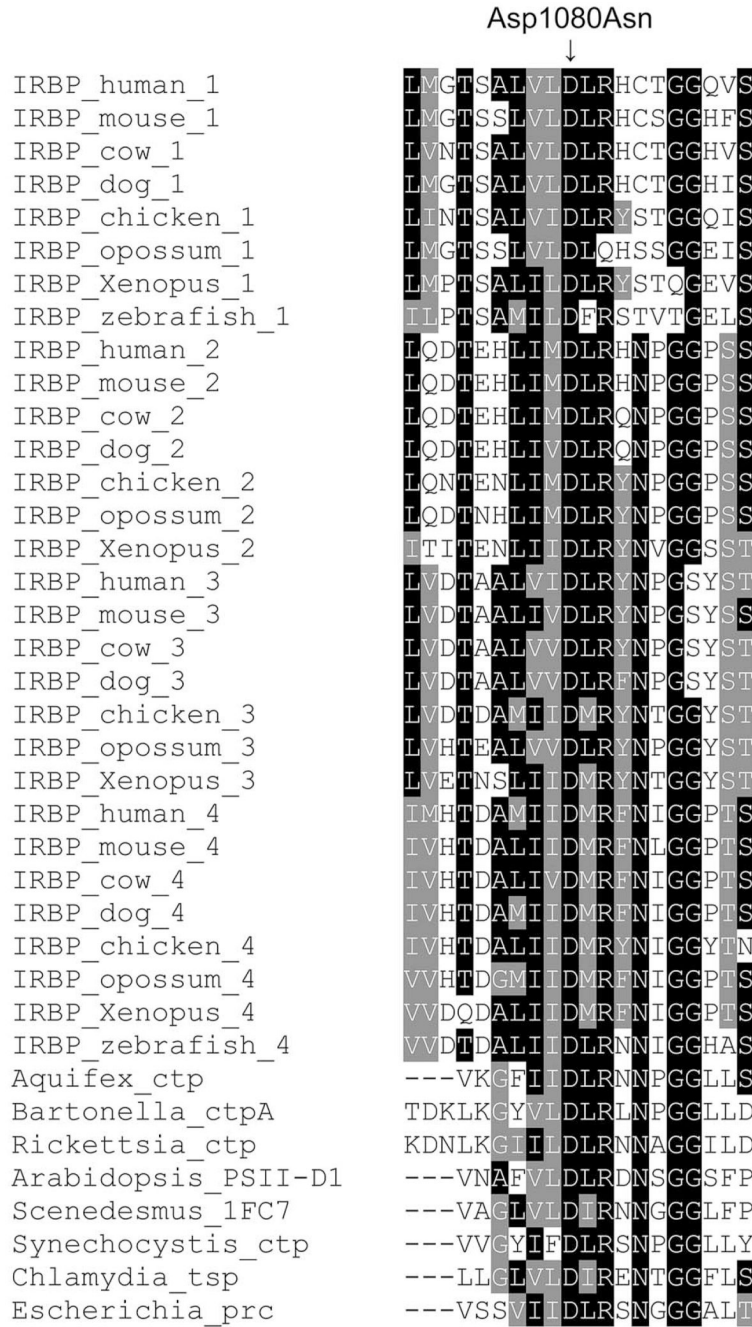
Figure 2.
Alignment of the four IRBP repeat modules of vertebrate species, and C-terminal-processing proteases of bacteria, algae, and plants. The black highlighting indicates identical residues, the gray highlighting indicates conserved residues, and no highlighting indicates residues that are not conserved. Asp1080 is a completely identical residue among all these sequences. The multiple sequence alignment was made with ClustalW using the Blosum scoring matrix, and shaded with BoxShade 3.21 (all provided in the public domain by the EMBnet, Swiss Institute of Bioinformatics, Lausanne, Switzerland, http://www.ch.embnet.org/index.html).
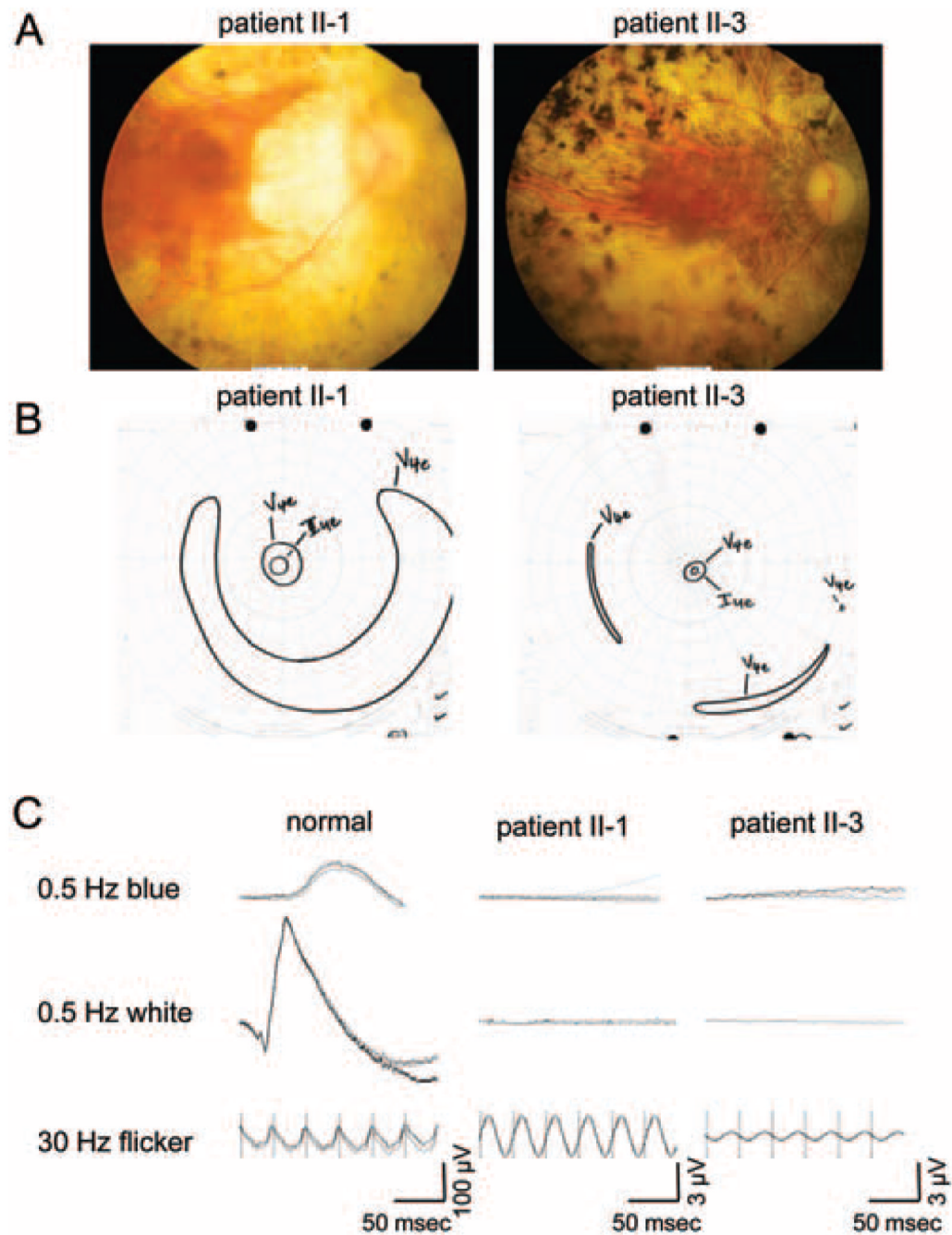
Figure 3.
Clinical characteristics of two affected siblings demonstrated variability in the severity of the disease. The older brother (II-1) was less severely affected than the younger brother was (II-3). (**A**) More clumped and bone spicule pigment was noted on ophthalmoscopy in the younger (*right*) versus the older (*left*) brother. (**B**) Visual fields of the right eyes of the patients are illustrated. Visual fields were more severely diminished in the younger brother (II-3; *right*) than in the older brother (II-1; *left*). (**C**) Full-field ERGs from both brothers (columns 2 and 3) reveal profound loss of rod function (0.5 Hz blue) and some remaining cone function (30-Hz flicker) compared with normal (column 1). The panels show the right eye of these patients at their most recent visits. Three consecutive sweeps are overlaid to illustrate ERG response

reproducibility, three successive responses to a flash of light, or, in the case of the cone, the flicker.
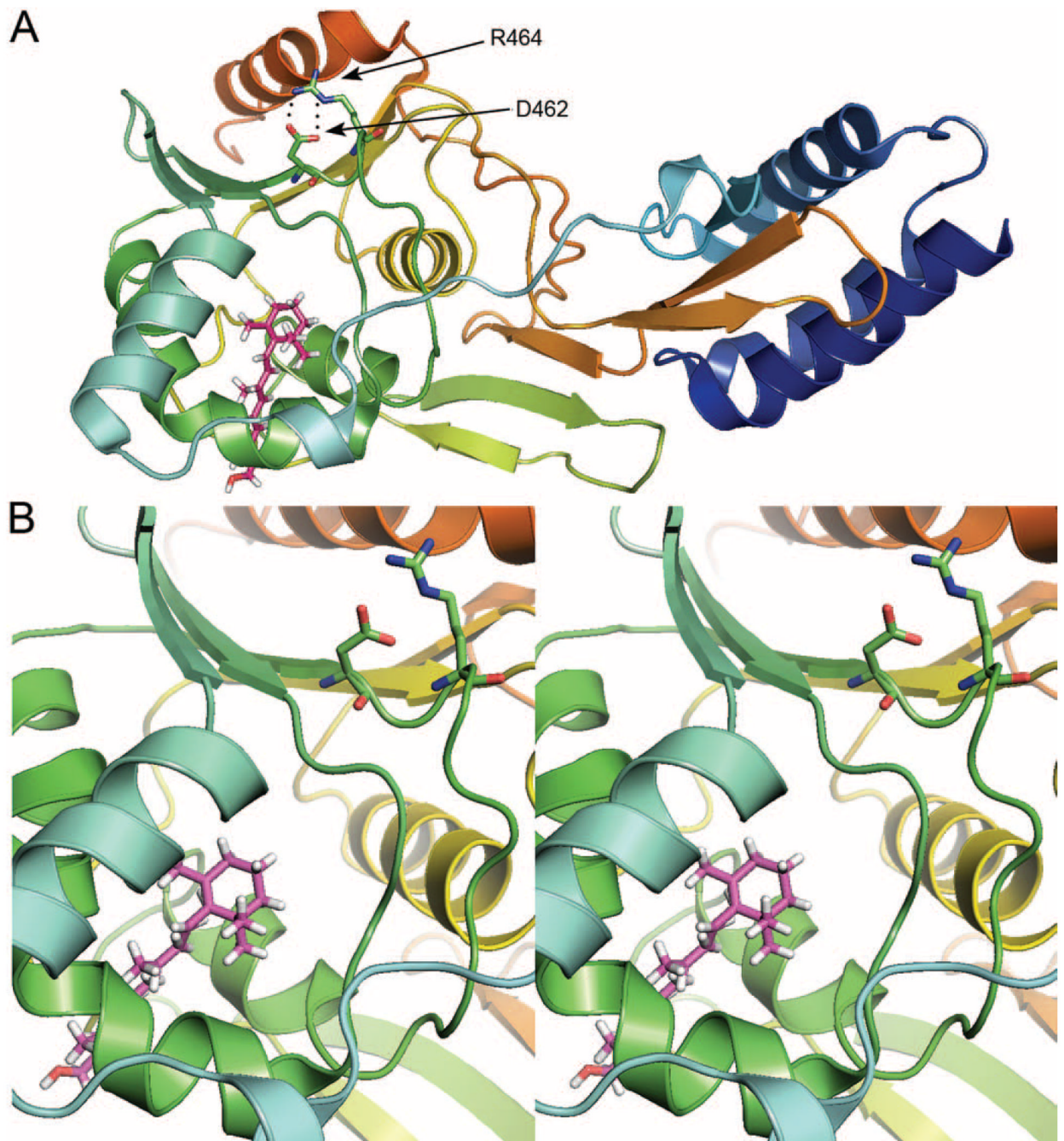
Figure 4.
Molecular modeling of the Asp1080Asn mutation. (**A**) Structural modeling suggests that the highly conserved aspartic acid (D) and arginine (R) residues form a salt bridge in the scaffold of the retinol-binding pocket. This ribbon structure represents the second module of *Xenopus* IRBP (X2IRBP) docked with all-*trans* retinol (carbons, *magenta*). *Blue*: the X2IRBP N-terminal region; *red*: C-terminal region. D462, the aspartic acid residue corresponding to D1080 in human IRBP, and R464 are shown in stick representation (oxygen, *red*; nitrogen, *blue*). A probable salt bridge forms between the carboxamide side group of D462 and guanidinium group of R464 (*dotted line*). (**B**) Stereo view showing the relationship between the retinol-binding pocket and the conserved D and R residues (The image may be viewed in

3-D without specialized stereo glasses. Suggestions for viewing molecular stereo images are found at http://spdbv.vital-it.ch/themolecularlevel/0help/stereoview.html).
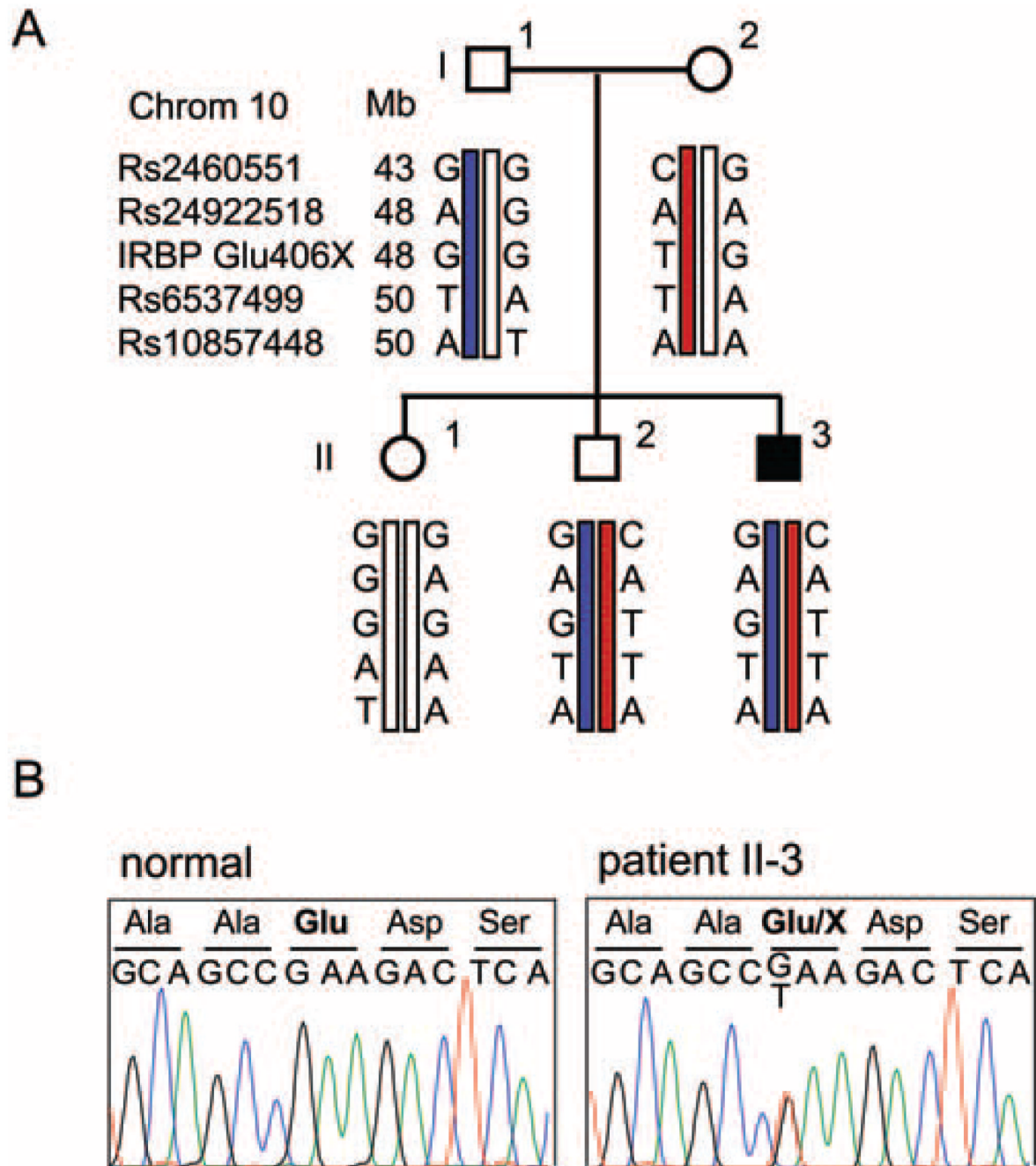
Figure 5.
Haplotype analysis in the family members of an isolate patient with sector RP. (**A**) A heterozygous nonsense mutation (c.1216G>T, p.Glu406X) was identified in the patient and in his unaffected brother, who carried the same haplotype on the other allele. (**B**) Sequence chromatogram showing the heterozygous nonsense mutation identified in this family.

TABLE 1

PCR Primer Pairs for RBP3

Exon	Size (bp)	Forward Primer (5′–3′)	Reverse Primer (5′–3′)
1 (a)	411	GCTTGCACACAGTCCAGGGA	TTGCAGCCAGGCAAGCAGTT
1 (b)	386	AGCACTCACCAGCCTCTCAG	TGGTGAGGACCACCACATC
1 (c)	570	GAAAGGTACGGTGCCGACAA	TGAGTCTTCGGCTGCAGCGT
1 (d)	356	CCACAGAAACTCCTTCTTGG	ATAGGTGGTGAAGAGGTGCA
1 (e)	428	TCCTACTTCCAGGGCCCTGA	AGGCTTTGGTGGAACTCCAG
1 (f)	499	GGACAAAGCCCAGGAAGTG	GTAGCTGCCAGGGTTGTAGC
1 (g)	405	CTGAACTGGAGACAGTGAAG	TGCTGCCCACCTGGTAGATG
1 (h)	471	GGAGGCGCACTCTCTGTGGG	GGGACTGGGTTCAGCCAGGT
2	326	TGCTTTCCTGGGCTCTAAAA	GCCCATAGCTTTGACTGTCC
3	293	CAAAGATCCTGGCCTCCC	CTGTCTTTCCCTGGTTTCCC
4	481	GCCCAGGCAGGATAGAGAAG	GTCCCAGAGGTTCTGTCTGC

TABLE 2

Clinical Characteristics of Patients II-1 and II-3

	Norm	Patient II-1				Patient II-3			
		67*		46*		52*		65*	
		OD	OS	OD	OS	OD	OS	OD	OS
Visual acuity	20/20	20/80	20/60	20/200	20/200	20/200	20/200	20/400	20/400
Refractive error (spherical equivalent)		−12.00	−14.00	−16.50	−17.00	−16.50	−17.00	Plano†	Plano†
Color vision		Normal		NA		Tritan Axis		NA	
Field area contiguous to the center (deg^2)	≥11310	339	494	333	307	139	67	82	103
Equivalent circular diameter contiguous to the center (deg)	≥120	21	25	20	20	13	9	10	11
Dark adaptation threshold elevation above normal (log units)		2.0		2.5		3.0		4.5	
ERG 0.5-Hz blue light (µV)	≥100	ND	ND	ND	ND	ND	ND	ND	ND
ERG 0.5-Hz white light (µV)	≥350	ND	ND	ND	ND	ND	ND	ND	ND
ERG 30-Hz white flicker (µV)	≥50	1.98	2.38	1.4	0.84	0.74	0.63	0.45	0.45
ERG 30-Hz white implicit time (ms)	≥32	40	38	45	43	48	41	56	52

NA, not available; ND, not detectable <10 µV without computer averaging.

* Age at visit (y).

† After lens implant.

TABLE 3

Synonymous Sequence Changes Detected in *RBP3* in 1075 Patients

Nucleotide	Amino Acid	arRP	iRP	adRP	CRD	LCA	Other
Alleles analyzed (*n*)		578	212	206	196	82	876
78C>T	Ser26Ser	1					
489C>T	Ser163Ser	1					
816C>A	Gly272Gly	2		1			
837G>A *	Thr279Thr*	58	23	13	9	4	60
843C>T	Pro281Pro	1	1	2			1
885G>T	Thr295Thr						1
924G>A	Pro308Pro	1					1
927C>T	Ala309Ala	1					
1044C>T	Pro348Pro	1					
1296G>A	Val432Val		1				
1401G>A	Pro467Pro	1					
1809C>T	Gly603Gly				1		
2016C>T	Ala672Ala				1		
2095T>C *	Leu699Leu*	9	1	3	3	1	2
2247C>T	Asp749Asp	5	1			1	7
2388C>G	Leu796Leu	1					
2742C>T	Pro914Pro	1					
2856T>C	Tyr952Tyr		1				1
2898C>T	Ser966Ser	9	4	4	1	1	12
3346C>T	His1182His	1					
3381G>A	Gln1127Gln						1
3471C>T	Ile1157Ile		1				
3546C>T	His1182His			1	1		

arRP, autosomal recessive RP; iRP, isolate RP; adRP, autosomal dominant RP.

*
Known SNP.

TABLE 4

Nonsynonymous Sequence Changes Detected in *RBP3* in 1075 Patients

Nucleotide	Amino Acid	arRP	iRP	adRP	CRD	LCA	Other
Alleles analyzed (*n*)		578	212	206	196	82	876
53G>T	Gly18Val						1
365G>A	Arg122His						1
463G>A	Val155Met	1					
487T>C*	Ser163Pro*					1	
586G>A	Val196Met						1
800G>A*	Arg267Gln*			1			
844G>A*	Val282Met*	1					
962C>T	Thr321Ile				1		
973G>A	Ala325Thr	1					
1037G>A	Arg346His	6	2	2		1	8
1135G>A	Ala379Thr						1
1216G>T*	Glu406X*		1				
1298C>T	Ser433Leu		1				
1327C>A	Arg443Ser						2
1514A>T	His505Leu	1					
1553A>G	Gln518Arg						1
1569C>G	His523Gln	1					
1603C>T	Arg535Cys			1			
1631G>A*	Arg544His*	3		1			2
1778T>C*	Val593Ala*			1			
1795A>G	Ile599Val		2				
1840G>A	Asp614Asn	1					
1844C>T	Ala615Val						1
2024C>T	Thr675Ile						1
2063C>T*	Ala688Val*			1			1
2077G>A	Val693Met	1	1			1	3
2168C>T	Pro723Leu	3					2

Nucleotide	Amino Acid	arRP	iRP	adRP	CRD	LCA	Other
2221G>A	Gly741Ser					1	
2239C>T*	Arg747Cys*	1					
2355C>A*	Asn785Lys*			1			
2497C>T*	Arg833Cys*	1		1			
2503G>A	Gly835Ser						1
2650G>A†	Val884Met†		1		1		
2708C>G	Thr903Arg	1					
2763C>A	Ser921Arg	1					
2866G>A	Glu956Lys		1				
2888C>T	Thr963Ile						1
3062C>A	Ser1021Tyr	1					
3175G>A	Val1059Ile		1				
3581C>T	Thr1194Met				1		1
3667C>G	Leu1223Phe		1				

Abbreviations as defined in Table 3.

*
Does not segregate with the disease.

†
Known SNP